# Vibration Analysis of Induction Motors with Unbalanced Loads

Selahattin GÜÇLÜ[1], Abdurrahman ÜNSAL[1] and Mehmet Ali EBEOĞLU[1]

[1]Dumlupinar University, Department of Electrical Engineering, Tavşanlı Yolu, 10. km. Kutahya/TURKEY
unsal@dpu.edu.tr, selahattin.guclu@dpu.edu.tr, mebeoglu@dpu.edu.tr

## Abstract

**One of the factors that cause the failure of induction motors which are used intensively in industry is the unbalanced loading of the motor. In this paper, a system to simulate the unbalanced loading condition of a three-phase squirrel cage induction motor was designed. The stator current and vibration signals of the motor were recorded. The vibration signals under balanced and unbalanced loading conditions were recorded with an accelerometer which was mounted on the motor housing. The stator current and vibrations signals were analyzed with Power Spectral Density (PSD). The results shows that the system can be used to simulate the effects of the unbalanced loading conditions of the induction motors.**

## 1. Introduction

One of the most-widely used electrical motors in modern industrial plants is the induction motor. Induction motors play an important role in the safe and efficient operation of industrial plants. Compared to other electric motors, induction motors have many advantages such as simplicity of their structure, high reliability, and relatively low cost. However, there is a possibility of faults when converting electrical energy to mechanical energy. Maintenance and fault diagnosis of induction motors are becoming increasingly important in the industry. Periodic inspection of induction motors and/or preventive maintenance are time-consuming and expensive. The detection of faults in induction motors is important in maintenance work. The detection of faults at an early stage is very important to prevent the total breakdown of the motors and/or processes. If the necessary measures are not taken at an early stage the failed induction motor may be replaced which leads to financial losses. Fault identification and diagnosis in a timely and regular manner can increase the reliability of the system and provide repair/replacement. Also the condition monitoring is important to avoid unexpected and catastrophic failures.

The faults of induction motors include stator winding failures, broken rotor bars, misalignment, static and/or dynamic air gap irregularities and bearing failures. The distribution of faults occurring in induction motors is given in Fig. 1.

The major faults of induction motors can broadly be classified is as follows:

a. Stator winding faults;
b. Broken rotor bars or end rings;
c. Static and/or dynamic air gap irregularities;
d. Shaft related faults;
e. Rotor winding faults;
f. Bearing faults.

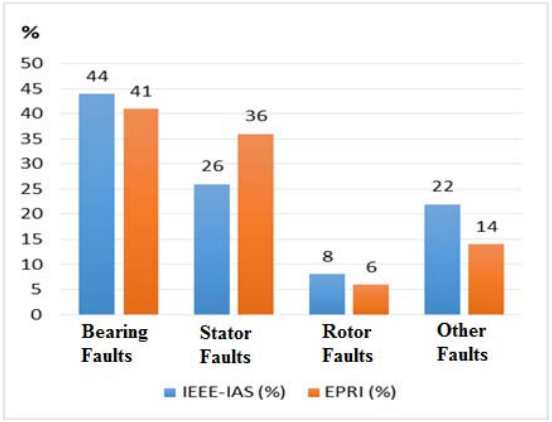


**Fig. 1.** Induction motor failures [1]

Mechanical faults of induction motors, such as rotor imbalance and misalignment of the shaft, are most common problems. In most applications, it is important to notice that these mechanical faults affect the safety and/or efficiency of working environment [2, 3].

Mechanical faults may cause torque oscillations and/or eccentricity faults. Torque oscillations may be caused by unbalanced loading, shaft misalignment, gearbox faults and bearing related faults. An eccentricity fault is a nonuniform air gap which may be caused by bearing wear or bearing failure, and bad motor assembly with unbalanced or noncentral rotor [4-7].

Eccentricity faults as shown in Fig. 2, are classified into three groups: static eccentricity (SE), dynamic eccentricity (DE) and mixed eccentricity (ME) [4, 7, 8] .

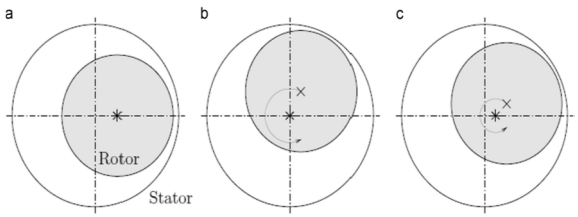


**Fig. 2.** Different types of eccentricity fault [5]

The eccentricity faults causes the sideband frequencies in the stator current and vibration signals of induction motors [5][9, 10]. These side-band frequencies can be calculated as

$$f_{ecc} = f_s \pm k f_r = f_s \left(1 \pm k \frac{(1-s)}{p}\right) \quad (1)$$

where fs is the supply frequency, k =1,2,3…, s is the slip, $f_r$ is the rotor speed frequency, and p is the number of pole pairs [11].

The side-band harmonics related eccentricity and the unbalanced loading conditions of the motor is found by using equations (1). This study is focused on the effects of unbalanced loading conditions which may eventually lead to eccentricity faults [5, 12, 13]. The unbalanced loading conditions of the motor was simulated by drilling a hole on the shaft of the motor and by mounting a stem through this hole. The effects of the unbalanced loading is investigated by the using the power spectral density (PSD) of stator current and vibrations signals. The PSD is described next.

### 1.1 Power Spectral Density

The extraction of the information in signals is accomplished by using the Power Spectral Density (PSD). In order to calculate PSD the signal is transferred to frequency domain by using discrete Fourier Transform then the PSD of the signal is calculated [14].

The discrete Fourier transform of sampled x(t) signal (with N samples) at frequency $m\Delta f$ is given by the following equation:

$$X(m\Delta f) = \sum_{k=0}^{N-1} x(k\Delta t) . \exp[-j2\pi km/N] \qquad (2)$$

where Δf is the frequency resolution and Δt is the sampling time interval;

The spectral density of the $x(t)$ sign is estimated as

$$S_{xx}(f) = \frac{1}{N} |X(m\Delta f)^2| \qquad (3)$$

### 1.2. The Unbalanced Loading System

The system to simulate the unbalanced loading of the induction motor is given in Fig. 3. A hole with an 8 mm diameter was drilled on shaft of the rotor. A stem with a length of 200 mm was mounted on the shaft as shown in Fig. 3. The stem has two nuts, one of them (on the end side) is used to adjust the degree of unbalance. The change in the degree of unbalance is realized by adjusting the distance "a" and "b" as shown in Fig. 3. When the degree of unbalance changes the amplitude of the resulted harmonics which are reflected in both the stator current and vibration signals changes accordingly.

In this study two different degrees of unbalanced conditions were simulated and tested. These two unbalanced conditions are given in Table 1.

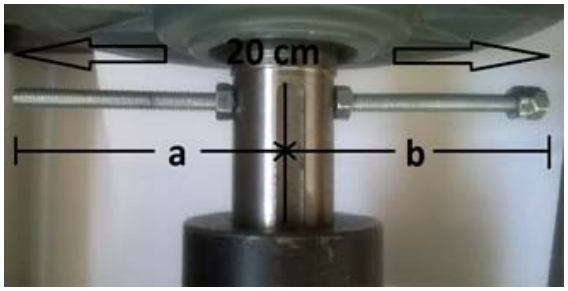


**Fig. 3.** The simulated unbalanced system

**Table 1.** Unbalanced conditions

| M = ma x h (force x force arm) | | |
|---|---|---|
| | a | b |
| Unbalance 1 | 94 | 106 |
| Unbalance 2 | 66 | 134 |

## 2. The Experimental Setup

The block diagram of experimental set-up is shown in Fig. 4. A 50 Hz, two poles three-phase 7.5 kW induction motor was used in the experiment. The induction motor was loaded with a synchronous generator. The output of the generator is connected to a 5 kW resistive load. The nameplate values of induction motor are shown in Table 2.

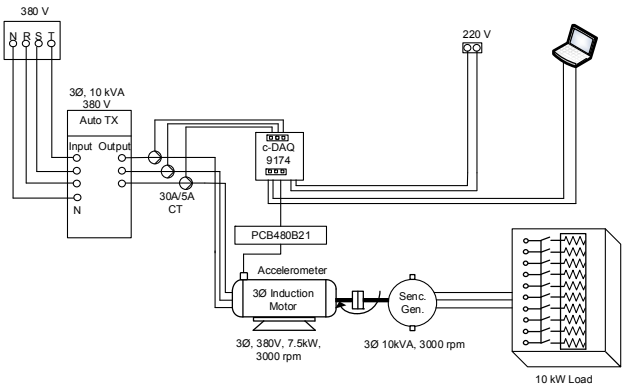


**Fig. 4.** The block diagram of experimental setup

Table 2. Nameplate of induction motor.

| | |
|---|---|
| Mark | GAMAK |
| Model | AGM2E 132 S 2b |
| Phase | 3 Phases |
| Power | 7,5 kW |
| Rotor Rotation Speed | 2910 rpm |
| Nominal Current | 13,6 A |
| Moment | 24,6 N |
| Number of poles | 2 |
| Power Factor | 0,90 |
| Efficiency | %88,5 |

The stator current and vibration signals of the induction motor were recorded by using The National Instrument (NI cDAQ-9174) data acquisition system. The stator current was recorded by using NI 9227 module. The vibration signals were recorded by using a triaxial accelerometer (PCB Piezotronics, 356A32). The output of the accelerometer is amplified by using an amplifier (PCB Piezotronics, 480B21). Fig. 5 shows the installation of the vibration accelerometer. The amplified signal is recorded by using using NI 9225 module. The sampling frequency of the data acquisition system was set to 25 kHz.

The motor under test was connected to power supply through an auto transformer. The experiments were realized under three different balance conditions: balanced, unbalanced 1, and unbalanced 2. In all three conditions the motor was run under

100% loading condition. The stator current and vibration signals were recorded by NI hardware and LabVIEW tool. The analysis of recorder data was carried out by using MATLAB.

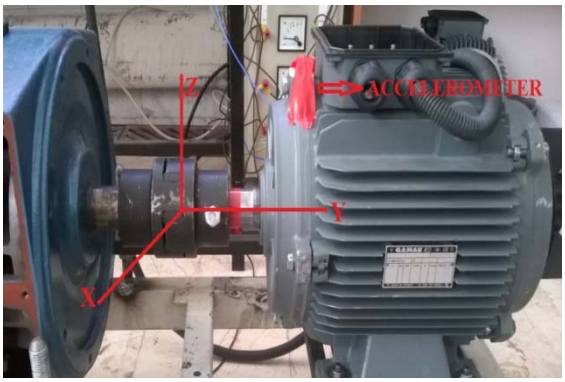


**Fig. 5.** Axes on the motor of the triaxial accelerometer

## 3. Results

The motor was tested under three different balance conditions. All three different balance tests were realized under 100% loading. Under all tests the stator current and vibration signals were recorded and analyzed to determine the characteristic frequencies of unbalance conditions of the motor. Fig. 6 shows the PSD of stator current of the motor under balanced loading condition. Fig. 7 and Fig. 8 indicate the PSD of the stator current under unbalanced 1 and unbalanced 2 respectively. The characteristic frequencies ($f_{vib}$) of side-band harmonics of stator current due to the unbalanced condition are 98,5 Hz and 147 Hz. The degree of unbalance in "unbalanced 1" condition is higher than the degree of unbalance in "unbalanced 2" condition. Therefore when the degree of unbalance increases the amplitude of the characteristic harmonics also increases (Fig. 6 -Fig. 8). This can be seen from Table 3 which shows the PSD of the stator current under different balance conditions. The amplitude and frequencies of the characteristic harmonics of the stator current are under "balanced", "unbalanced 1" and "unbalanced 2" are given in the Table. When the degree of unbalance increases the amplitude of the side-band harmonics also increases.

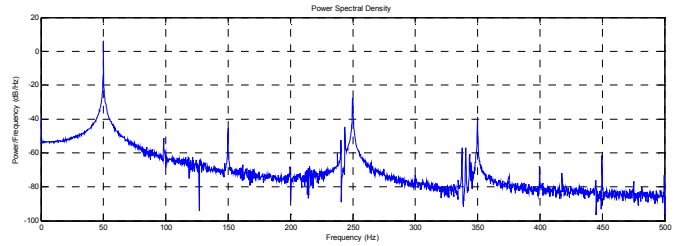


**Fig. 6.** The PSD of the stator current (under balanced condition)

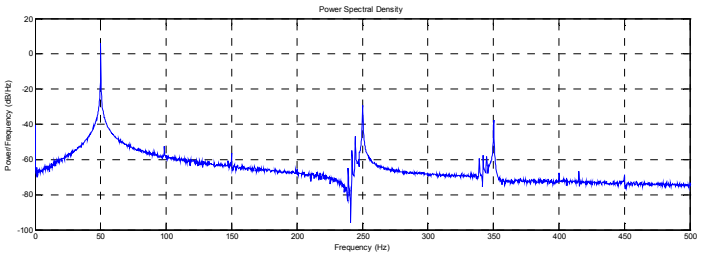


**Fig. 7.** The PSD of the stator current (under unbalance 1 condition )

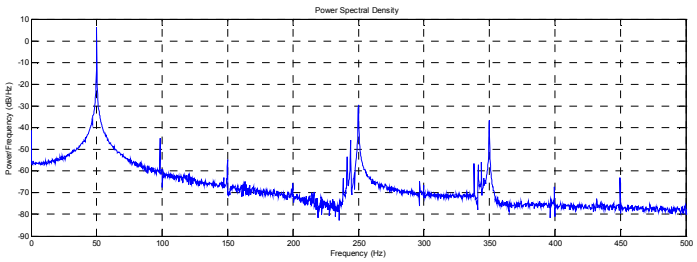


**Fig. 8.** The PSD of the stator current (under unbalanced 2 condition)

**Table 3.** Calculation of the $f_{vib}$ values of stator current data according to motor load conditions and amplitude values

| $F_{vib}=(f_s \pm k.f_r)Hz$ | $f_s$-$f_r$ | | $f_s$+$f_r$ | | $f_s$+2$f_r$ | |
|---|---|---|---|---|---|---|
| Theoretically calculated values | 1,5 | | 98,5 | | 147 | |
| Measured values | $F_{vib}$ (Hz) | Amplitude value (dB/Hz) | $F_{vib}$ (Hz) | Amplitude value (dB/Hz) | $F_{vib}$ (Hz) | Amplitude value (dB/Hz) |
| Balanced Loading | - | - | 98,5 | -51,19 | 150 | -45,44 |
| Unbalanced 1 Loading | - | - | 98,75 | -52,6 | 150 | -56,28 |
| Unbalanced 2 Loading | - | - | 98,5 | -44,74 | 150 | -54,89 |

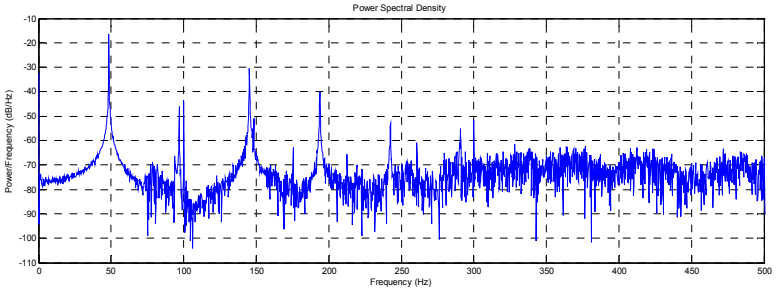


**Fig. 9.** PSD of y-axis vibration signal (under balanced condition)

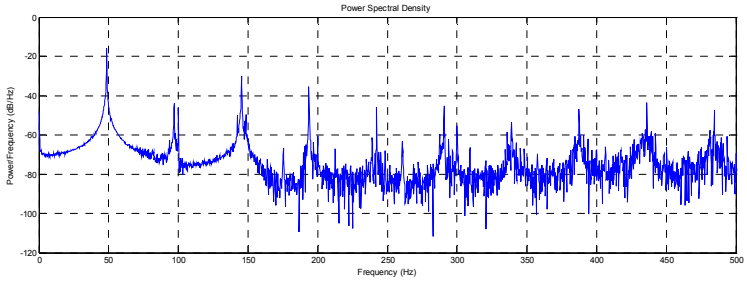


**Fig. 10.** PSD of y-axis vibration signal (under unbalanced 1 condition)

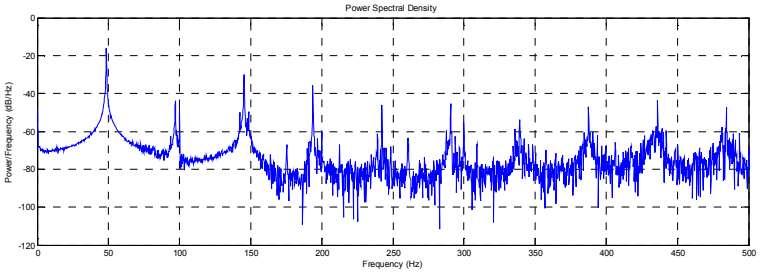


**Fig. 11.** PSD of y-axis vibration signal (under unbalanced 2 condition)

The three-axis vibration signals were analyzed by applying PSD. The characteristic frequencies of vibration under balanced and unbalanced loading conditions of the motor were analyzed. Since the amplitude of the vibration frequencies in the y-axis and z-axis is higher than the amplitude of the vibration frequency in the x-axis direction only the y-axis and z-axis vibration signals are shown in this study. Fig. 9, Fig. 10, and Fig. 11 show the PSD of the y-axis vibration signal under "balanced", "unbalanced 1" and "unbalanced 2" conditions respectively. Similarly, Fig. 12, Fig. 13, and Fig. 14 show the PSD of the z-axis vibration signal under "balanced", "unbalanced 1" and "unbalanced 2" conditions respectively. The characteristic frequencies ($f_{vib}$) of side-band harmonics of the vibration due to the unbalanced conditions are 98,5 Hz and 147 Hz. The degree of unbalance in "unbalanced 1" condition is higher than the degree of unbalance in "unbalanced 2" condition. When the degree of unbalance increases the amplitude of the characteristic harmonics of the vibration also increases (Fig. 9 -Fig. 14). This can be seen from Table 4 which shows the PSD of the vibration signals under different balance conditions. The amplitude and frequencies of the characteristic harmonics of the vibration signals under "balanced", "unbalanced 1" and "unbalanced 2" are given in the Table. When the degree of unbalance increases the amplitude of the side-band harmonics also increases. Table 4 shows the PSD of the vibration signals under different balance conditions.

**Table 4.** Calculation of the $f_{vib}$ values of vibration data according to motor load conditions and amplitude values

| $F_{vib}=(f_s \pm k.f_r)Hz$ | | $f_s-f_r$ | | $f_s+f_r$ | | $f_s+2f_r$ | |
|---|---|---|---|---|---|---|---|
| Theoretically calculated | | 1,5 | | 98,5 | | 147 | |
| Measured values | | $F_{vib}$ (Hz) | Amplitude value (dB/Hz) | $F_{vib}$ (Hz) | Amplitude value (dB/Hz) | $F_{vib}$ (Hz) | Amplitude value (dB/Hz) |
| Balanced Loading | X | 0,5 | -75,15 | 97 | -34,75 | 145,5 | -43,36 |
| | Y | 1 | -73,56 | 97 | -46,03 | 145,5 | -30,61 |
| | Z | 0,5 | -69,78 | 97 | -46,19 | 145,5 | -30,14 |
| Unbalanced 1 Loading | X | - | - | 97 | -37,08 | 145,3 | -42,52 |
| | Y | - | - | 97 | -43,9 | 145,3 | -30,01 |
| | Z | - | - | 97 | -43,42 | 145,3 | -28,99 |
| Unbalanced 2 Loading | X | - | - | 96,75 | -33,78 | 145,3 | -37,16 |
| | Y | - | - | 96,75 | -34,39 | 145,3 | -29,08 |
| | Z | - | - | 96,75 | -32,78 | 145,3 | -28,05 |

## 4. Conclusions

In this study, an induction motor was tested under three different balance conditions under 100% loading. The unbalanced conditions which can easily be seen from PSD of the stator current and vibration signals may eventually cause dynamic eccentricity in the induction motor. The calculated $f_{vib}$ values were compared with the measured values. The change of the amplitude value x-axis, y-axis, and z-axis vibration signals clearly indicate the unbalanced condition of the motor. The motor was tested under different balance conditions. When the degree of the unbalance changes (from balanced to "unbalance 1" to "unbalance 2") the amplitude of the side-band harmonics of stator current and vibrations signals changes (increases) accordingly.

**Acknowledgments:** This research was funded by Dumlupinar University Research Fund (DPÜ-BAP 2016-71).

## 5. References

[1] K. S. Khadim Moin Siddiqui, V.K.Giri, "Health-monitoring-and-fault-diagnosis-ininduction-motor-a-review," *International Journal of Advanced Research in Electrical, Electronics and Instrumentation Engineering,* vol. 3, no. 1, January 2014.

[2] P. A. Delgado-Arredondo, D. Morinigo-Sotelo, R. A. Osornio-Rios, J. G. Avina-Cervantes, H. Rostro-Gonzalez, and R. d. J. Romero-Troncoso, "Methodology for fault detection in induction motors via sound and vibration signals," *Mechanical Systems and Signal Processing,* vol. 83, pp. 568-589, 2017.

[3] T. G. H. Ramzy R. Obaid, David J. Gritter, "A Simplified Technique for Detecting Mechanical Faults using Stator Current in Small Induction Motors," *0-7803-6401-5/00/$10.00 Q 2000 IEEE*.

[4] M. Blodt, J. Regnier, and J. Faucher, "Distinguishing Load Torque Oscillations and Eccentricity Faults in Induction Motors Using Stator Current Wigner Distributions," *IEEE Transactions on Industry Applications,* vol. 45, no. 6, pp. 1991-2000, 2009.

[5] J. Faiz and S. M. M. Moosavi, "Eccentricity fault detection – From induction machines to DFIG—A review," *Renewable and Sustainable Energy Reviews,* vol. 55, pp. 169-179, 2016.

[6] T. G. H. Xianghui Huang, "Detection of Mixed Air Gap Eccentricity in Closed-Loop Drive-Connected Induction Motors," *07803-7838-5/03/$17.W 82003 IEEE*.

[7] M. Blodt, M. Chabert, J. Regnier, and J. Faucher, "Mechanical Load Fault Detection in Induction Motors by Stator Current Time-Frequency Analysis," *IEEE Transactions on Industry Applications,* vol. 42, no. 6, pp. 1454-1463, 2006.

[8] M. Blodt, P. Granjon, B. Raison, and G. Rostaing, "Models for Bearing Damage Detection in Induction Motors Using Stator Current Monitoring," *IEEE Transactions on Industrial Electronics,* vol. 55, no. 4, pp. 1813-1822, 2008.

[9] V. Hegde and G. S. Maruthi, "Experimental investigation on detection of air gap eccentricity in induction motors by current and vibration signature analysis using non-invasive sensors," *Energy Procedia,* vol. 14, pp. 1047-1052, 2012.

[10] S. Nandi, H. A. Toliyat, and X. Li, "Condition Monitoring and Fault Diagnosis of Electrical Motors—A Review," *IEEE Transactions on Energy Conversion,* vol. 20, no. 4, pp. 719-729, 2005.

[11] Mohamed El Hachemi Benbouzid, "A Review of Induction Motors Signature Analysis as a Medium for Faults Detection," *IEEE Transactions On Industrial Electronics, Vol. 47, No. 5, October 2000*.

[12] S. Karmakar, S. Chattopadhyay, M. Mitra, and S. Sengupta, "Induction Motor and Faults," pp. 7-28, 2016.

[13] B. K. L. Caryn M. Riley, Thomas G. Habetler, and Randy R. Schoen, "A Method for Sensorless On-Line Vibration Monitoring of Induction Machines," *IEEE Transactions On Industry Applications, Vol. 34, No. 6, November/December 1998*.

[14] M. U. Emine Ayaz, Serhat Seker, and Belle R. Upadhyaya, "Signal Based Fault Detection for Stator Insulation in Electric Motors," *04651641*.